Degenerate four-wave mixing with a tunable excimer laser

Michel Versluis, Gerard Meijer, and David W. Chandler

We use a simple, forward-geometry degenerate four-wave mixing setup to monitor weak absorptions of various gas-phase molecules with a tunable excimer laser. With this technique, state-selective detection of H_2, CO, H_2O, and O_2 is demonstrated. The dependence of the forward-geometry degenerate four-wave mixing signals on various experimental parameters (e.g., pressure, laser power) is determined. Several mechanisms for the generation of the observed signals are discussed, including diffraction from density gratings or thermal gratings and two-photon degenerate four-wave mixing.

1. Introduction

Degenerate four-wave mixing (DFWM) has been demonstrated as a sensitive technique to monitor gas-phase species.[1-6] The technique has been applied to radicals such as OH and NH, in which transitions to electronic states are easily accessible. Here we demonstrate a DFWM experiment that uses a tunable excimer laser to state-selectively detect weak gas-phase transitions in H_2, CO, H_2O, and O_2. The ability to detect all of these species sensitively makes this technique a promising diagnostic tool for many combustion environments. This technique is one of a host of gas-phase grating experiments that are being developed to measure background-free gas-phase absorptions. Related gas-phase grating-based techniques were recently demonstrated by Buntine et al.[7] and Zhang et al.[8] Buntine's technique, termed two-color laser-induced grating spectroscopy, uses nondegenerate light pulses and requires multiple resonances in the molecule. This research was recently extended to the study of both two-photon transitions[9] and dissociating molecules.[10] Zhang's technique is also a double-resonant technique in

which an excitation laser precedes a DFWM scheme so that DFWM can be carried out from the excited state.

Earlier DFWM experiments[1-6] showed the applicability of the DFWM technique in flames and combustion environments. These experiments were done by using the backward-geometry detection scheme. Phase-conjugate mirrors could then be used to maintain the coherence properties of the grating-generating beams, even in turbulent environments. Our forward-geometry detection scheme does not possess this phase-conjugate property. Recent experiments by Fourkas et al.[11] showed that transient grating experiments in flames could be performed with an experimental geometry similar to the one we use.

These DFWM and grating-based techniques complement laser-induced fluorescence, direct absorption, and ionization detection schemes. The techniques are quite sensitive and rely solely on the absorption process; the detected molecules do not have to radiate or ionize in order to be detected. Additionally, the signal comes out as a coherent light beam and can be detected in a zero-background manner in a location remote from the interaction region. Similar techniques have been used to study optical phase conjugation[12-15] and to detect transient absorptions in liquids.[16,17]

Here we report the use of a simple, foward-geometry degenerate four-wave mixing (DFWM-FG) arrangement[18,19] as a way to monitor weak absorptions of stable molecules in the gas phase by using a tunable excimer laser. In particular we demonstrate the detection of H_2 by means of the $E, F\ ^1\Sigma_g^+$ $(v' = 6, 7) \leftarrow X\ ^1\Sigma_g^+\ (v'' = 0)$ two-photon transition, the detection of CO by means of the one-photon spin-forbidden singlet-triplet transition $a\ ^3\Pi\ (v' = 2) \leftarrow X$

When this work was performed M. Versluis and G. Meijer were with the Department of Molecular and Laser Physics, University of Nijmegen, Toernooiveld, NL-6525 ED Nijmegen, The Netherlands. M. Versluis is now with the Molecular Dynamics Laboratory, Faculty of Science and Technology, Griffith University, Nathan, Brisbane, Qld, Australia 4111. D. W. Chandler is with the Combustion Research Facility, Sandia National Laboratories, Livermore, California 94550.

$^1\Sigma^+$ ($v'' = 0$), the detection of O_2 by means of the B $^3\Sigma_u^-$ ($v' = 4$) $\leftarrow$ X $^3\Sigma_g^-$ ($v'' = 0$) (Schumann–Runge band) transition, and the detection of H_2O by means of the two-photon $\tilde{C}$ $^1B_1 \leftarrow \tilde{X}$ $^1A_1$ transition. Although the origin of the diffracted signals may change for each system, these spectra demonstrate the sensitivity and utility of using the tunable excimer laser in the DFWM-FG arrangement as a way to monitor these important combustion and atmospheric species. We have determined the dependencies of the DFWM-FG signals obtained in H_2 on both the pressure of the probed gas and the pressure of the foreign gas. Laser-power dependencies are determined as well.

2. Degenerate Four-Wave Mixing in Forward Geometry

DFWM can be explained both in a nonlinear optics picture, in terms of an induced nonlinear polarization and the third-order susceptibility tensor $\chi(3)$, and in a dynamic grating picture. Both pictures are being used concurrently.[17,20] For reasons of clarity, the grating picture will be used here. The experimental evidence for the generation of density gratings, discussed in Subsection 4.B, supports the choice of the more elucidating and pedagogical grating picture. The apparatus used for performing the DFWM spectroscopy in the DFWM-FG technique described here is schematically represented in Fig. 1. A mask is placed in the excimer laser beam with 2-mm holes located at three corners of a rectangle to define three parallel coherent laser beams. The three beams are crossed in a cell containing the sample by being focused through a single lens. At the intersection of the beams, interference of two of the beams creates a periodically varying spatial intensity distribution of light. If the wavelength of the beams is resonant with an absorption in the gas sample, then a spatial distribution of excited molecules, a grating, is created. The grating period Λ, equivalent to the grating fringe spacing, is determined by the wavelength λ_p of the coherent laser beams that creates the grating and the crossing angle ϑ between the intefering beams[17]:

$$\Lambda = \lambda_p/2 \sin(\vartheta/2). \quad (1)$$

A third laser beam of wavelength λ_c focused at the interaction region in the cell is diffracted off of the grating. The diffracted beam comes out of the sample
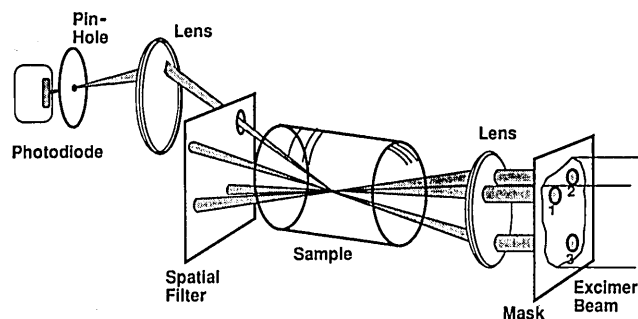

Fig. 1. Schematic view of the experimental setup for a DFWM-FG experiment.

toward the fourth corner of the rectangle (behind the focus). The diffraction of the probe beam can be described as a Bragg reflection in which the following condition holds:

$$\sin \alpha = m\lambda_c/2\Lambda = m \sin(\vartheta/2)\lambda_c/\lambda_p$$
$$= m \sin(\vartheta/2), \quad m = 1, 2, \ldots. \quad (2)$$

The deflected beam (λ_c) is degenerate in wavelength with the two beams setting up the grating (λ_p), and it is automatically phase matched if the holes in the mask are chosen as described. The crossing angle of the two laser beams that form the grating is ϑ, the exit angle of the signal beam is α, and m is the order of the diffraction. For a thick grating that has a sinusoidal intensity pattern (i.e., one-photon transition and no saturation of the transition), the first-order diffraction ($m = 1$) is the only order that is phase matched and observed. The reflectivity of the grating is determined by the total number of probed grooves, hence by the combination of the groove spacing and the spatial overlap of the beams. For a given geometry of the three input laser beams, a long focal length lens makes a grating with larger groove spacings than a grating created with a shorter focal length lens, because of the shallower crossing angle. If diffusion is the mechanism for destruction of the grating, it will persist longer when formed with the larger groove spacing.

It is important to note that gratings will be set up in the medium by various combinations of the incoming beams. From inspection of Fig. 1, we see that beams 2 and 3 will set up a grating to which beam 1 is phase-matched, and thus part of beam 1 will be deflected through the spatial filter onto the detctor. Similarly, beams 1 and 2 will set up a grating off of which part of beam 3 will deflect onto the detector, although the diffraction will not be as strong because of the larger angle of incidence. A third grating, set up by beams 1 and 3, deflects beam 2 at a different angle and is not detected in this geometry. Note that beam 2 takes part in the creation of both of the gratings that are detected.

3. Experimental

In the DFWM-FG experiments described here, a line-narrowed tunable excimer laser (Lambda Physik, EMG 150 MSCT) is used as the radiation source. Operating on ArF at 193 nm, the laser has a linewidth of approximately 1.0 cm^{-1}. The laser is tunable from 51,600 to 51,850 cm^{-1}. The ArF laser output energy is approximately 50 mJ per pulse and this energy is homogeneously distributed in a 7 mm $\times$ 22 mm rectangular-shaped beam. Running on KrF at 248 mm, the laser has an output of approximately 150 mJ, in a 0.5-cm^{-1} line, tunable from 40,200 to 40,350 cm^{-1}. The beam dimensions of the KrF excimer laser are almost identical to those of the ArF laser. The tunable excimer laser has a tuning range of approximately 1 nm, which is an obvious limitation for doing spectroscopy. However, many important

combustion species can be detected by using these spectrally bright lasers (CO, H_2, H_2O, OH, NO, and O_2).

The laser radiation is coherent enough over the beam cross section that three parallel coherent beams can be formed by sending the main laser beam through a mask. The use of unstable resonator optics in the amplifier of the excimer laser is required to generate this coherence. So far, no DFWM-FG signals have been recorded with the laser in the amplified oscillator mode.[21] Most pulsed dye lasers have incoherent properties over their beam cross section. Therefore, when using a dye laser, one can generate a grating most efficiently by splitting the dye laser beam with beam splitters and by focusing the split beams separately. To ensure maximum coherence, one must make sure that each light beam travels the same distance to the crossing region. This again shows an important advantage of the application of tunable excimer lasers with this simple geometry to this field of spectroscopy.

The mask, positioned 5 cm behind the amplifier's output coupler, consists of three 2.0-mm-diameter holes in an aluminum plate. The holes are located on three corners of a rectangle that has sides of 4.0 and 10.0 mm. The position of the mask in the laser beam is adjusted so that the energy per pulse of the three secondary beams is approximately equal. The energy of the three individual laser beams is 1 mJ per pulse at maximum. In some experiments a stack of two or three masks is used to prevent stray light from the primary excimer laser beam from interfering with the signal beam. The three laser beams are focused with a 50-mm-diameter, 30-cm focal length lens, passing a quartz window of a stainless-steel cell filled at subatmospheric pressures (typically between 10 and 300 mbars) with the gases under investigation. An iris diaphragm behind the cell spatially filters the DFWM-FG signal beam, located at the fourth (dark) corner of the rectangle, from the main laser beams. A lens–pinhole–lens arrangement is set up to minimize stray light further. A 50-μm pinhole is used in most cases. The signal beam is detected with either a photodiode detector (Lambda Physik, LF 302 UV) or with a photomultiplier tube detector (EMI 9635 QB).

The experiments on O_2 and H_2O are partly performed in room air at a pressure of 1 bar. With H_2O in ambient air (typical Dutch humidity), the DFWM-FG signal is intense enough to be traced by eye by means of its blue fluorescence on a piece of white paper, even with the room lights on. The signal from the photodetector is fed into a boxcar integrator, and the 10- or 30-shot averaged output is displayed on a strip-chart recorder. None of the spectra shown here are normalized to laser power.

4. Results and Discussions

A. Molecular Spectra

In the upper panel of Fig. 2, the DFWM-FG spectrum of the spin-forbidden one-photon transition from the
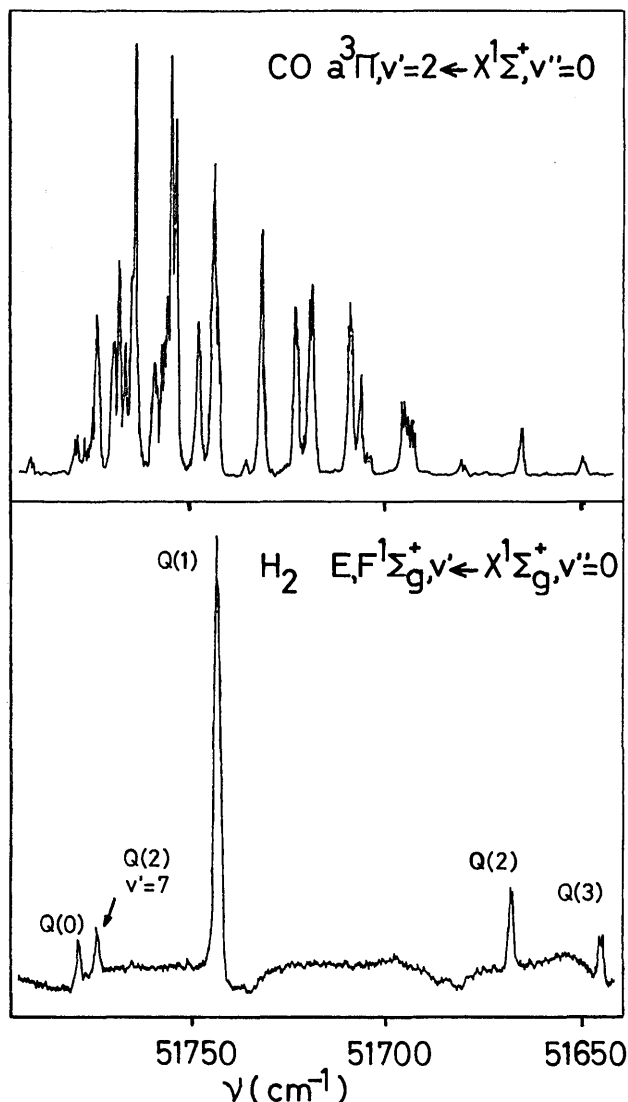

Fig. 2. DFWM-FG spectra of the spin-forbidden $a\ ^3\Pi$ ($v' = 2$) ← $X\ ^1\Sigma^+$ ($v'' = 0$) transition in 300 mbars of CO and of the two-photon E, $F\ ^1\Sigma_g^+$ ($v' = 6, 7$) ← $X\ ^1\Sigma_g^+$ ($v'' = 0$) transition in 50 mbars of H_2, measured with a tunable ArF excimer laser.

$X\ ^1\Sigma^+$ ($v'' = 0$) state to the metastable $a\ ^3\Pi$ ($v' = 2$) state in CO is shown. The assignments of all the individual lines in the spectrum, as well as a simulation of the expected line intensities, are given in Meijer et al.[22] A direct comparison of the observed and theoretically expected line intensities is somewhat difficult. First, a spectral fluctuation in the intensity of the locked (i.e., narrow-band) laser power over the ArF gain profile exists. In addition, near 51,790 cm^{-1}, narrow-bandwidth laser operation ceases completely as a result of an intracavity metastable C-atom absorption.[23] Second, some well-known rotational lines in the $v' = 4$ ← $v'' = 0$ band of the Schumann–Runge system of O_2 absorb the laser light between the laser head and the detector.[24] Nevertheless, a qualitative comparison of the DFWM-FG spectrum shown here with the theoretically predicted spectrum for CO at 300 K (Ref. 22)

shows a reasonable correspondence between observed and calculated line intensities. The CO spectrum shown here has been recorded with 300 mbars of CO in the cell, but even with the photodiode detector the CO spectra could be measured at pressures down to 10 mbars. At 300 mbars of pressure the spectrum remains optically thin so that the signal beam is not attenuated as it leaves the sample cell.

In the lower panel of Fig. 2, the DFWM-FG spectrum of the two-photon $E, F\ ^1\Sigma_g^+$ ($v' = 6, 7$) $\leftarrow X\ ^1\Sigma_g^+$ ($v'' = 0$) transition in 50 mbars of H_2 is shown. The four lowest Q-branch transitions to the $v' = 6$ level, as well as the $Q(2)$ transition to the $v' = 7$ level, lie within the tuning range of the ArF laser.[25-27] A small nonresonant background signal is visible in the spectrum. One possible explanation is that the background is produced by diffraction from a grating of ions produced by a direct near-resonant three-photon ionization of the H_2. The dips in this broad signal are due to the absorption of the laser light on its way to the detector by the aforementioned O_2 resonances. Spectra similar to the one shown here have been obtained by using either (2 + 1) resonance-enhanced multiphoton ionization (REMPI) with total ion-current detection[24] or two-photon excited laser-induced fluorescence.[26]

The question remains as to the mechanism responsible for the observed signal. One possible mechanism is the two-photon analog of the DFWM experiments, which is degenerate eight-wave mixing. This is a high-order process and would therefore be expected to be weak. Because of the strength of the signal and the power dependence that is discussed below, we do not believe that our signal is due to a degenerate eight-wave mixing process. A more likely explanation is that the process producing the signal beam is not from diffraction from a stationary grating but rather from a resonance-enhanced difference-frequency mixing mechanism,[28-34] in which the resonance occurs at the two-photon step and the output beam is identical in frequency to the input beam. A four-wave mixing signal produced in this manner would be identical to the one observed but would be of lower order and therefore stronger. It should be noted that this process is not described by a grating picture, because the entire medium contributes to the signal. This contribution makes the signal more robust for diagnostic purposes. The signal strength will decay with the collisional dephasing rate but not with the grating diffusion rate. Recently[35] a tunable variant of this mechanism was published in which an excimer laser was used to excite the same two-photon transition in H_2, and in which a second tunable laser beam was used to stimulate the emission of a vacuum UV photon.

For H_2 a second-order signal beam [$m = 2$ in Eq. (2)] is also visible (i.e., diffracted at twice the incident angle), even at a pressure of 50 mbars. The H_2 spectrum measured by this second-order deflection shows more nonlinear line intensities. Although there are several mechanisms that would lead to

second-order diffraction, including degenerate six-wave mixing and saturation of the grating, we have no conclusive evidence of the origin of this signal.

We have obtained molecular spectra of O_2 and H_2O by focusing the three excimer laser beams in room air. The O_2 DFWM-FG signal is obtained by focusing the 193-nm ArF excimer laser beam in air. The predissociative $B\ ^3\Sigma_u^-$ ($v' = 4$) $\leftarrow X\ ^3\Sigma_g^-$ ($v'' = 0$) Schumann–Runge band transitions of O_2 (Ref. 24) are detected. The line intensities in the observed spectrum are somewhat distorted because much of the laser light (including the signal beam) is absorbed by the oxygen resonances in the beam path. Superimposed on the broad $B \leftarrow X$ O_2 transitions, unassigned sharp transitions of either O_2 or O_2^+ are observed. These resonances have also been observed by using laser-induced fluorescence.[36,37]

Figure 3 shows the spectrum obtained when the KrF (248-nm) excimer laser is scanned over the H_2O $\tilde{C}\ ^1B_1 \leftarrow \tilde{X}\ ^1A_1$ transition. When excited to the $\tilde{C}\ ^1B_1$ state, some of the H_2O predissociates and thus forms OH in the $A\ ^2\Sigma^+$ state, and some is ionized to form H_2O ions. This H_2O transition has been observed and assigned by Meijer et al.[38] by using (2 + 1) REMPI-detecting H_2O ions as well as the detection of OH $A\ ^2\Sigma^+$ state emission as a function of the laser frequency. The transition has also been observed by using the two-photon excited fluorescence of the H_2O molecule.[39] Meijer et al.[38] determined the photodynamics of the predissociation, ionization, and fluorescence processes when this state of H_2O is excited. The spectrum obtained by monitoring the OH $A\ ^2\Sigma^+$ state emission as the photolysis laser wavelength is scanned is very different from our DFWM-FG spectra.
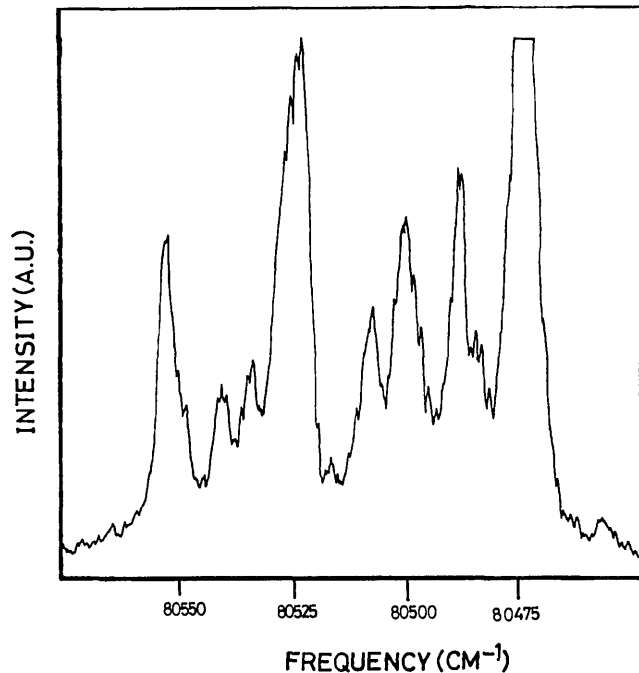

Fig. 3. DFWM-FG spectrum of the H_2O $\tilde{C}\ ^1B_1 \leftarrow \tilde{X}\ ^1A_1$ transition in ambient air taken with a tunable KrF excimer laser. The peaks are all assigned in Ref. 31.

The DFWM-FG spectrum we observe is nearly identical to the aforementioned (2 + 1) REMPI spectrum and the parent molecular fluorescence excitation spectra. One possible explanation is that the grating probed in this experiment is a density grating formed from the difference in the total number of H_2O molecules or H_2O^+ ions. The probed grating is clearly not composed of regular population differences of the OH photoproducts. A more likely explanation is that the process producing the signal beam is the same as that which was hypothesized for the H_2 signal, which was resonance-enhanced difference-frequency mixing. We believe that this is a useful way to observe many two-photon transitions.

B. Forward-Geometry Degenerate Four-Wave Mixing Pressure Dependence

To quantify the origin of the observed four-wave mixing processes, we determine the pressure dependencies of the DFWM-FG signals in H_2. Figure 4 shows the pressure dependence of the four-wave mixing signal of pure H_2. The pressure in the cell is varied between 10 and 200 mbars. The curve in Fig. 4 corresponds to a cubic pressure dependence and fits the data remarkably well. The experiment is repeated for pure CO, for which a cubic pressure dependence is also found. In the CO experiment the pressure is varied from 20 to 550 mbars.

To check the influence of the background pressure on the signal, we fill the cell with 50 mbars of H_2. Helium is added as a foreign gas, and the total pressure is varied while we monitor the DFWM-FG signal. The measured dependence is shown in Fig. 5. Here a clear linear behavior is observed, indicating the presence of a collision-induced thermal (or
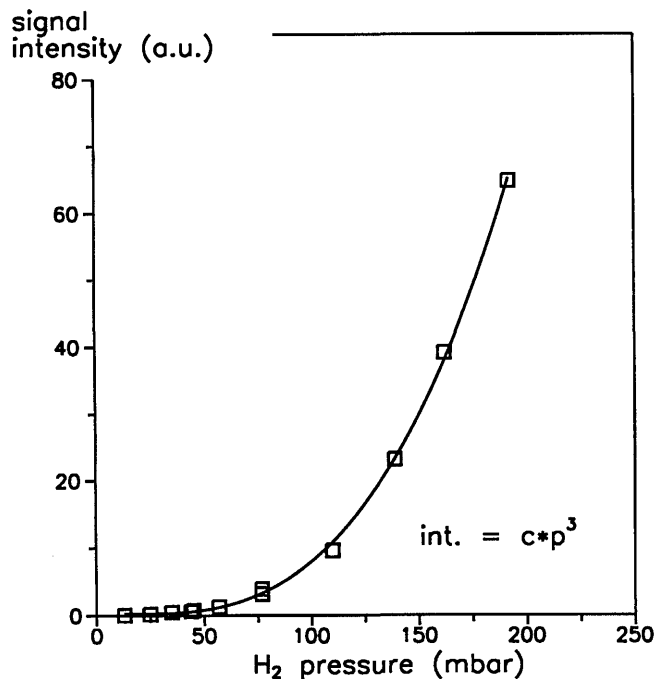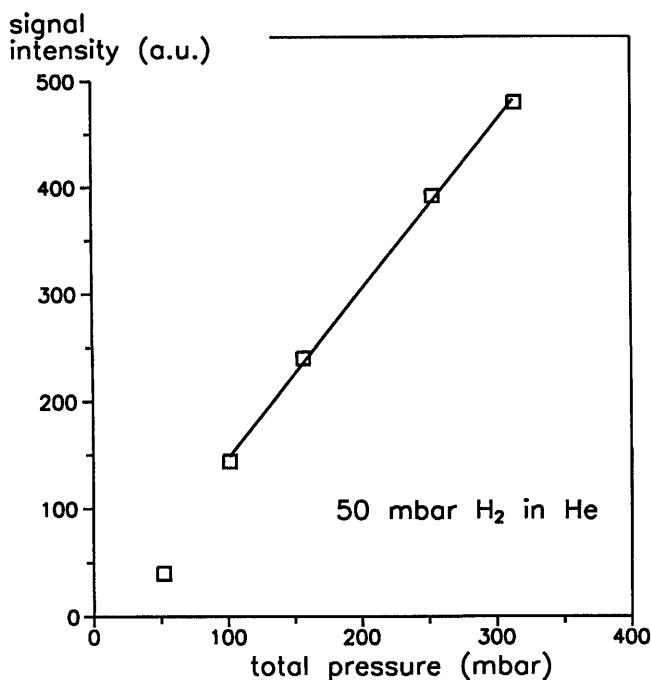

Fig. 5. Pressure dependence of the DFWM-FG signal in H_2 if helium is added as a foreign gas. A linear dependence is found.

density) grating. A thermal grating is formed by the difference in temperature between where the molecules have been excited and collisionally relaxed and where they have not. The difference in temperature creates a density grating that scatters the probe laser beam. The lowest data point has not been included in the fit because only H_2–H_2 collisions are relevant at this pressure. From the two experiments above, we conclude that at pressures above approximately 10 Torr a density grating is generated by a collisional process in the sample during the pulse duration of the laser. This density grating is produced by collisional energy transfer from the excited H_2; as the pressure increases, the number of collisions increases during the laser pulse, and more energy is transferred into the sample. Additionally, the higher pressure leads to a slower diffusion rate, which maintains the density grating and increases the scattering efficiency.

In the H_2 experiments the DFWM signal grows quadratically with the density of the probed molecule, as is the case for four-wave mixing processes such as DFWM and coherent anti-Stokes Raman spectroscopy. However, at the higher pressures of our experiment, we know that part of that enhancement is due to the formation of a density grating. The fact that the signal increases rather than decreases with pressure makes the technique complementary to existing diagnostic techniques, such as laser-induced fluorescence and REMPI, which work better at lower pressure as a result of collisional quenching of the fluorescence and the reduction of the mean-free path of the electrons and ions at atmospheric pressures, respectively. However, this technique must be better characterized before quantitative measurements can be attempted.
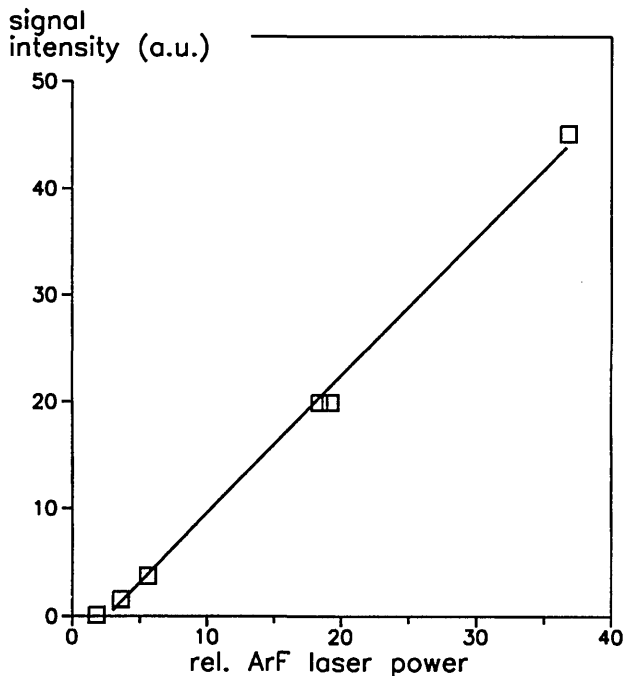

Fig. 4. H_2 pressure dependence of the DFWM-FG signal. A cubic dependence is found.

int. = $c*p^3$

signal intensity (a.u.)

rel. ArF laser power

Fig. 6. Laser-power dependence of the DFWM-FG signal in H_2. The power of the three beams is attenuated simultaneously.

C. Forward-Geometry Degenerate Four-Wave Mixing Laser-Power Dependence

The intensity patterns observed for the two-photon absorption in H_2 and H_2O appear to have very similar relative intensities as the corresponding $(2 + 1)$ REMPI spectra of the same transitions. The observed spin-forbidden one-photon transition in CO has approximately the intensity of the calculated transition strengths. We measured the DFWM-FG signal dependence on the total laser power and found a linear dependence of over 1 order of magnitude (see Fig. 6). This indicates that we are well into the saturation regime, even for our lowest laser powers. Even if the transition is completely saturated by the grating-writing beams, the signal beam should increase linearly with total laser power because of linear dependence of the signal on the probe laser intensity.

Conclusions

We have shown that the DFWM-FG technique can be used to detect weak transitions in H_2, CO, H_2O, and O_2 molecules. The mechanisms for the production of the signal are speculative. This research complements research by others on the detection of radicals that uses similar techniques. We have determined the pressure and power dependencies of the DFWM-FG signals in H_2. We conclude that for H_2, under our relatively high-pressure conditions, the signal we measure comes partially from a density grating formed from collisions. The production of density gratings makes the DFWM-FG technique more sensitive at higher pressures, which makes this single-laser technique complementary to existing diagnostic tools.

References

1. P. Ewart and M. Kaczmarek, "2-D mapping of temperatures in a flame by DFWM in OH," Appl. Opt. **30**, 3996–3999 (1991).
2. P. Ewart and S. V. O'Leary, "Detection of OH in a flame by DFWM," Opt. Lett. **11**, 279–281 (1986).
3. T. Dreier and D. J. Rakestraw, "Measurement of OH rotational temperatures in a flame using DFWM," Opt. Lett. **15**, 71–74 (1990).
4. T. Dreier and D. J. Rakestraw, "DFWM diagnostics on OH and NH radicals in flames," Appl. Phys. B **50**, 479–483 (1990).
5. D. J. Rakestraw, R. L. Farrow, and T. Dreier, "2-D imaging of OH in flames by DFWM," Opt. Lett. **15**, 709–711 (1990).
6. R. L. Farrow and D. J. Rakestraw, "Detection of trace molecular species using degenerate four-wave mixing," Science **257**, 1894–1900 (1992).
7. M. A. Buntine, D. W. Chandler, and C. Hayden, "A 2-color laser-induced grating technique for gas-phase excited state spectroscopy," J. Chem. Phys. **97**, 707–710 (1992).
8. Q. Zhang, S. A. Kandel, T. A. W. Wasserman, and P. H. Vaccaro, "Detection of stimulated emission pumping via DFWM," J. Chem. Phys. **96**, 1640–1643 (1992).
9. J. A. Gray, J. E. M. Goldsmith, and R. Trebino, "Detection of atomic hydrogen by two-color laser-induced grating spectroscopy," Opt. Lett. **18**, 444–446 (1993).
10. T. J. Butenhoff and E. A. Rohlfing, "Laser induced gratings in free jets. I. Spectroscopy of NO_2," J. Chem. Phys. **98**, 5460–5468 (1993); "Laser induced gratings in free jets. II. Photodissociation dynamics via photofragment, transient gratings," **98**, 5469–5476 (1993).
11. J. T. Fourkas, T. R. Brewer, H. Kim, and M. D. Fayer, "Picosecond polarization-selective transient grating experiments in sodium-seeded flames," J. Chem. Phys. **95**, 5775–5784 (1991).
12. R. A. Fischer, ed., Optical Phase Conjugation (Academic, New York, 1983).
13. D. M. Pepper, "Non-linear optical phase conjugation," Opt. Eng. **21**, 155–156 (1982).
14. M. Ducloy, "Nonlinear optical phase conjugation," in Advances in Solid State Physics, P. Gross Aschen, ed. (Pergamon, New York, 1982).
15. T.-Y. Fu and M. Sargent III, "Theory of two-photon conjugation," Opt. Lett. **5**, 433–435 (1980).
16. M. D. Fayer, "Dynamics of molecules in condensed phases: picosecond holographic grating experiments," Ann. Rev. Phys. Chem. **33**, 63–87 (1982).
17. H. J. Eichler, D. Pohl, and P. Gunter, Laser-Induced Dynamic Gratings, Vol. 50 of Springer Series in Optical Sciences (Springer, New York, 1986).
18. G. M. Carter, "Excited state dynamics and temporally resolved non-resonant non-linear optical processes in polydiacetylenes," J. Opt. Soc. Am. B **4**, 1018–1024 (1987).
19. W. Du, X. Zhang, K. Chen, Z. Lu, Y. Zheng, and J. Wu, "Multiple forward phase conjugate waves by degenerate four-wave mixing in Langmuir–Blodgett films with BOXCARS geometry," Opt. Commun. **84**, 205–207 (1991).

20. Y. R. SHEN, "Basic considerations of 4-wave mixing and dynamic gratings," IEEE J. Quantum Electron. **QE-22**, 1196–2403 (1986).

21. M. Versluis, M. Ebben, M. Drabbels, and J. J. ter Meulen, "Frequency calibration in the ArF excimer laser tuning range using laser-induced fluorescence of NO," Appl. Opt. **30**, 5229–5234 (1991).

22. G. Meijer, A. M. Wodtke, H. Schlüter, P. Andresen, H. Voges, "State-selective detection of CO using a tunable excimer laser," J. Chem. Phys. **89**, 2588–2589 (1988).

23. M. Versluis and G. Meijer, "Intra-cavity C atom absorption in the tuning range of the ArF laser," J. Chem. Phys. **96**, 3350–3351 (1992).

24. D. M. Creek and R. W. Nicholls, "Comprehensive re-analysis of the O_2 Schumann–Runge band system," Proc. R. Soc. London Ser. A **341**, 517–523 (1975).

25. L. M. Hitchcock, G. S. Kim, E. W. Rothe, and G. P. Reck, "Stimulated Raman pumping of H_2 $(v'' = 1, J'' = 1)$ and REMPI from it using a single laser," Appl. Phys. B **52**, 27–31 (1991).

26. T. Okada, M. Maeda, Y. Kajiki, K. Muraoka, and M. Akazaki, "Sensitive detection of H_2 molecules by 2-photon excited LIF," Appl. Phys. B **43**, 113–116 (1987).

27. D. J. Kliger and C. K. Rhodes, "Observation of 2-photon excitation of H_2 $E, F\, {}^1\Sigma_g{}^+$ state," Phys. Rev. Lett. **40**, 309–312 (1978).

28. G. C. Bjorklund, "Effects of focusing on third-order nonlinear processes in isotropic media," IEEE J. Quantum. Electron. **QE-11**, 287–296 (1975).

29. C. R. Vidal, "Coherent VUV sources for high resolution spectroscopy," Appl. Opt. **19**, 3897–3903 (1980).

30. R. Hilbig and R. Wallenstein, "Tunable VUV radiation generated by two-photon resonant frequency mixing in xenon," IEEE J. Quantum Electron. **QE-19**, 194–201 (1983).

31. S. D. Kramer, C. H. Chen, M. G. Payne, G. S. Hurst, and B. E. Lehmann, "Tunable VUV light generation for the low-level resonant ionization detection of krypton," Appl. Opt. **22**, 3271–3275 (1983).

32. N. Georgiev, U. Westbloom, and M. Alden, "Detection of CO molecules using two-photon degenerate four wave mixing (DFWM)," Opt. Commun. **94**, 99–102 (1992).

33. D. G. Steel and J. F. Lam, "Two-photon coherent transient measurement of the nonradiative collisionless dephasing rate in SF6 via doppler free degenerate four-wave mixing," Phys. Rev. Lett. **43**, 1588–1591 (1979).

34. J. A. Gray and R. Trebino, "Two-photon four-wave mixing spectroscopy of atomic hydrogen in flames," submitted to Chem. Phys. Lett.

35. C. E. M. Strauss and D. J. Funk, "Broadly tunable difference-frequency generation of VUV using two-photon resonance in H_2 and Kr," Opt. Lett. **16**, 1192–1194 (1991).

36. G. Laufer, R. L. McKenzie, and W. M. Huo, "Radiative processes in air excited by an ArF laser," Opt. Lett. **13**, 99–101 (1988).

37. M. Versluis, "Combustion diagnostics at atmospheric pressures using a tunable excimer laser," Ph.D. dissertation (University of Nijmegen, Nijmegen, The Netherlands, 1992), p. 57.

38. G. Meijer, J. J. ter Meulen, P. Andresen, and A. Bath, "Sensitive quantum state selective detection of H_2O and D_2O by $(2 + 1)$ REMPI," J. Chem. Phys. **85**, 6914–6922 (1986).

39. A. Hodgson, J. P. Simons, M. N. R. Ashfold, J. M. Bayley, and R. N. Dixon, "Quantum state selected photodissociation dynamics in H_2O and D_2O," Mol. Phys. **54**, 351–368 (1985).